GeoStruct Innovations
https://www.acadlore.com/journals/GSI

Numerical Investigation of Short Anchor Cable Preload and Length on Surrounding Rock Stress and Stability

Rejoice Shumba[1], Rui Wu[1,2*], Bayoundoula Jefferson[3]

[1] School of Mining Engineering, Jiangxi University of Science and Technology, 341000 Ganzhou, China
[2] Jiangxi Provincial Key Laboratory of Safe and Efficient Mining of Rare Metal Resource, 341000 Ganzhou, China
[3] Collaborative Innovation Center for Development and Utilization of Rare Metal Resources Co-sponsored by Ministry of Education and Jiangxi Province, 341000 Ganzhou, China

[*] Correspondence: Rui Wu (wurui@jxust.edu.cn)

Received: 01-03-2025 **Revised:** 03-06-2025 **Accepted:** 03-21-2025

Citation: R. Shumba, R. Wu, and B. Jefferson, "Numerical investigation of short anchor cable preload and length on surrounding rock stress and stability," *GeoStruct. Innov.*, vol. 3, no. 1, pp. 37–51, 2025. https://doi.org/10.56578/gsi030104.

Abstract: Underground roadway excavation fundamentally alters the in-situ stress state of surrounding rock, often leading to stress redistribution, deformation, and plastic failure, which can compromise stability if not properly supported. This paper systematically examines the impact of short anchor cable preload and length on the stress distribution, the deformation behaviour, and the plastic zone development of numerical simulations in FLAC3D. A surrounding rock was modelled with an elastic-plastic Mohr-Coulomb constitutive model, and a single-variable parametric approach was used to isolate preload (150–350 kN) and cable length (2900–3700 mm) effects. Findings suggest that augmenting preload causes a significant decrease in maximum tensile stress, displacement and plastic zone depth, and an increase in compressive stress; but improvements plateau beyond 250 kN. Correspondingly, longer cable length results in better confinement of the rocks and decreased deformation, optimal results were achieved at 3300 mm, after which the benefits are marginal. In the study, a preload of 250 kN with a cable length of 3300 mm is found as the optimal configuration to stabilise the surrounding rock and ensure both economical and construction efficiency. These results offer quantitative data on the prestressed anchor mechanisms, which can be used to give real-life information on the design of underground support. In the future, field validation and variable geology conditions should be incorporated into the work as a means of further streamlining the support optimisation.

Keywords: Short anchor cable; Preload; Cable length; Plastic zone; Rock mass deformation; FLAC3D

1 Introduction

Underground roadways, in their excavation, essentially change the in-situ stress state of the host rock, and can cause extensive redistribution of stress and resultant deformation in the mass of the surrounding rock [1]. When tunnelling is performed, the displacement of the material will destroy the balance of stress initially, resulting in tensile and compressive stress concentrations around the opening that has been excavated, which may lead to crack propagation and localised failure unless properly supported. These stress variations act on geological discontinuities, joints or bedding planes, and increase the rate of displacement and plastic deformation in weak or heterogeneous rock masses as shown in recent numerical and experimental studies. The most frequent stability issues encountered during excavation include failure of the roof and spalling of the sidewalls, along with the overconvergence, which occur under high stress or complicated geological conditions.

The behaviour of the surrounding rock mass in response to such disturbances is essential in understanding not only the structural integrity of the tunnel projects but also maximising the design of the support and the safety of construction. The stress distribution, deformations and progression of failure are critical aspects which can be studied through detailed analyses to provide insights that are used to design effective support systems depending on the specific geotechnical environment [2]. The excavation process of the tunnel changes fundamentally the pre-existing stress field in the host rock, resulting in a major redistribution of stresses surrounding the opening. When the rock is removed, the balance between the existing in situ stresses is disrupted, and tensile stresses start to appear along the edges of the tunnel, whereas compressive stress concentrates in the adjacent areas, which can surpass the strength of the rock, and thus lead to failure [3].

This redistribution of stress normally creates an elastic zone around the tunnel, with the plastic and damaged zones that surround the rock and undergo permanent deformation. In these areas, the microcracks develop and extend under the control of disturbed stress and eventually aggregate into macro scale fractures that eventually characterise the failure modes as spalling, shear bands, or slab detachment [4]. The tensile, compressive, and shear stress interactions are highly dependent on excavation geometry such as circular or horseshoe tunnel profile has a different pattern of stress concentration and sequence of excavation, which influences the pattern of unloading and crack progress [5]. The ability to know these mechanical responses is essential in the design of efficient support systems since it offers an understanding of deformation process and the space time evolution of the failure of rocks around underground openings [6].

Anchor cable systems are important in the stabilisation of the surrounding rock within underground excavations to actively control the stress field within the post excavation and by limiting the deformation of the rock. When a tunnel is excavated, the instantaneous release of in situ stress can easily result in stress concentrations and massive displacements of the surrounding rock. Prestressed anchor cables provide an active tensile force to the rock mass, which complements compressive stress around the perimeter of the excavations and neutralises the negative implications of stress redistribution. The preloading of the cables causes the surrounding rock to move towards a more stable stress state and thus decreases tensile stress and inhibits the spread of fractures. This is an active mechanism of redistribution of stress that is a leading cause in managing deformation and postponing rock failure, especially in weak or jointed rock masses where deformation is otherwise pronounced.

As demonstrated through numerical research, it has been revealed that prestressed cable systems can considerably decrease plastic zone expansion and total convergence in terms of the passive methods to support these kinds of materials, finally unreinforced shotcrete or rock bolts [7]. They develop internal compressive arch, which enhances the load bearing capacity and reduces displacement, through mobilisation of the natural strength of the rock mass. This dynamic support system is more effective than the traditional low prestress systems, especially in deep or high stress areas, and prestressed anchor cables are now favored in the design of temporary supports of tunnels [8].

In prestressed support systems, the amount of preload and the actual length of the anchor cables have a critical effect on the mechanical reaction of the surrounding rock mass. Preload provides a initial tensile force, which dynamically involves the tensile support of the anchor cable when redistributing the stresses after an excavation minimises tensile zones and maximises compressive stress transfer at the rock support interface. High preload is more effective in mobilising the rock mass surrounding the tunnel perimeter, minimising the formation of plastic failure zones and reducing displacement but excess prestress can also cause underlying premature yielding of the anchor or unwarranted construction costs without optimisation. Conversely, a lack of preload cannot provide the desired effect of reinforcement leading to increased plastic areas and increased deformation under similar geological conditions.

The length of cable controls the power of reinforcement: the longer the cable is, the more the volume of rock it covers, introducing the effect of confinement, and the later it can induce failure zones, but the shorter the cable is, it may not be able to cover the plastic zone, reducing the support efficiency. Numerical simulation parametric studies have revealed that moderate preloads, which are accompanied by sufficient cable length, can contribute significantly to stability and do not lead to cost inefficient over design [9]. This optimisation is important in the design of useful support schemes in diverse geologic environments.

Recent design principles to support the anchor cable in tunnelling and underground excavations are largely based on empirical rules or simplified analytical techniques based on historical field experience and case studies [10]. Prescriptive recommendations on anchor spacing, length and preload are found in standards like the Chinese Code on Tunnel Support Design and other international practices according to rock quality designation (RQD) or other geological classification indices. Although such guidelines are useful in practical applications when used in routine applications, they may fail to take into consideration the nuanced, site dependent interactions between prestress magnitude, cable length, and the nonlinear behaviour of the surrounding rock mass under different stress conditions. Consequently, these empirical methods can result in conservative designs which end up raising project costs or under designed support schemes which undermine the stability in tough geological conditions [11].

This limits the ability to individually determine the effect of each parameter on the stress distribution, deformation, and plastic zone development [12]. This gap has been identified by recent studies, which have suggested that systematic, single variable studies are needed to better measure how preload or length affects rock response. In the absence of these focused studies, support parameters optimisation is mostly a matter of heuristics, highlighting the importance of detailed numerical and experimental research. Although the use of anchor cable support remains a common technique in underground engineering, research and design practices provide only minimal information about the contributions of preload magnitude and cable length to the behaviour of surrounding rocks [13].

Most of the previous investigations have combined these parameters into composite indices of support or used ad hoc formulations which fail to separate out their respective mechanical contributions in the presence of different stresses. This gap limits the accuracy of support design and may lead to either excessive conservatism or insufficient stability control in complex geological settings [14]. The objective of the research is to investigate the effect of short anchor cable preload and length systematically on stress redistribution, deformation characteristics, and the formation of plastic zones in the rock surrounding the tunnel through an elaborate numerical simulation. With the adoption of a single variable parametric analysis, this study gives detailed information about the distinctive influence of each parameter on rock behaviour. The novelty of the work is in the decreased deformation plasticity relationships quantified in a more focused way, allowing more reliable and cost-effective optimisation of support parameters.

This paper is organised in such a way that it presents a methodical examination of short anchor cable support within underground roadways. After this introduction, Section 2 provides the numerical modelling framework and simulation design, including the approach, support configuration and evaluation indicators. Section 3 contains the results and analysis of the study including stress redistribution, deformation behaviour and plastic zone development during different preload and cable lengths. Section 4 provides a discussion of the findings, combining the findings with previous literature and practical implications. Lastly, the study is concluded in Section 5 with a summary of main findings, design suggestions, and future research directions, which provides a logical roadmap of academic and engineering applications.

2 Materials and Methods

2.1 Numerical Modelling Approach

In this research, FLAC3D was selected as the chosen numerical simulation tool to determine the mechanical behaviour of surrounding rock and reinforcement effect of short anchor cable support in excavation of a roadway [15]. Due to its clear solution scheme and strong structural element interaction, FLAC3D has seen extensive use in the recent years in the analysis of tunnel and roadway stability and support optimisation studies in recent years. It is based on the explicit finite difference method (FDM), which solves the governing dynamic equilibrium equation in incremental form:

$$\rho \frac{d^2 u_i}{dt^2} = \frac{\partial \sigma_{ij}}{\partial x_j} + b_i \tag{1}$$

where, ρ is the material density, u_i represents displacement components, σ_{ij} is the stress tensor, and b_i denotes body forces.

The surrounding rock mass was modelled with an elastic-plastic constitutive model that is based on the Mohr-Coulomb failure and adequately represented shear failure as well as tensile cracking due to stress redistribution by the excavation. The shear yield criterion is expressed as:

$$f_s = \tau - c - \sigma_n \tan \phi = 0 \tag{2}$$

where, τ is shear stress, c is cohesion, σ_n is normal stress, and ϕ is the internal friction angle. Tensile failure is governed by:

$$f_t = \sigma_3 - \sigma_t = 0 \tag{3}$$

where, σ_3 is the minimum principal stress and σ_t is the tensile strength. Plastic zones develop once either criterion is satisfied. The model assumes homogeneous and isotropic behavior within each stratigraphic layer [16]. The rock mass in each stratigraphic layer was homogeneous and isotropic, the time-dependent process of creep and water-rock interaction were not considered. The experiment was performed in quasi-static and non-dynamic loading [17].

2.2 Geological Conditions and Model Geometry

The numerical model was designed to make a typical underground roadway section, and excavation geometry was set based on realistic engineering diagrams. The roadway uses a traditional arched-rectangular shape to mimic the regular nature of underground excavation forcing stress redistribution and deformation properties to be representative of field conditions. To reduce the influence of the boundary effects on the simulation results, the overall model size was determined to be at least several times larger than the span of the roadway by the rule that the model boundaries should be placed at least five times farther than the excavation width away the opening [18]. Appropriate boundary conditions were used to represent in-situ constraints. The in-situ stresses were initially imposed before excavation. The vertical stress was calculated using gravitational loading:

$$\sigma_v = \gamma H \tag{4}$$

where, γ is the unit weight of the overlying strata and H is burial depth. Horizontal stress was imposed using a lateral pressure coefficient:

$$\sigma_h = k\sigma_v \tag{5}$$

where, k represents the ratio of horizontal to vertical stress. Geological conditions were used to separate the surrounding rock mass into different layers of geological stratification. The mechanical parameters associated with each layer were given, such as the elastic modulus E, the ratio of Poisson v, cohesion c, the angle of friction ϕ, and tensile strength σ_t and density ρ [19].

2.3 Short Anchor Cable Support Configuration

The short anchor cables were installed around the roadway perimeter to enable active reinforcement of the surrounding rock. Cables were fitted at the roof and upper sidewalls at preset distance and inclination to achieve effective confinement in the shallow fractured zone [20]. In FLAC3D, anchor cables were represented by built-in structural cable constituents that can transmit axial forces to the enveloping rock mass. Preload was implemented through imposing an initial tension on the elements of the cable, which In FLAC3D, anchor cables were modelled using one-dimensional structural cable elements capable of carrying axial load only. The axial force along the cable is governed by:

$$F = EA\frac{du}{dx} \tag{6}$$

where, E is the elastic modulus of the cable material, A is the cross-sectional area, and du/dx is axial strain. Prestressing was simulated by applying an initial axial force P_0, such that:

$$F_{\text{total}} = P_0 + EA\frac{du}{dx} \tag{7}$$

The mechanism of active support of field-installed prestressed cables is reproduced in this formulation. The relations between the anchoring cables and the rock mass were modelled by using the coupling springs to convey the load and take into account the deformation against the anchorage length [21]. The relationship between shear transfers is:

$$\tau = k_s\Delta u \tag{8}$$

where, k_s is the bond stiffness and Δu is the relative motion between the cable and rock mass. Short anchor cables are more constructible than long cables and have been demonstrated to be effective in stabilising small plastic areas in moderate in-situ stress conditions [22].

2.4 Simulation Scenarios and Control Strategy

In numerical simulations, a single-variable control strategy was used to systematically assess the effect of the parameters of the anchor cables on roadway stability. This method enables the isolation of the mechanical effect of specific parameters and the limitation of the interplay of other aspects and is broadly used in parametric tests of underground support systems. There were two sets of simulation scenarios. The length of the anchor cable was maintained constant in the preload analysis, with preload levels of 150, 200, 250, 300 and 350 kN applied to study their influence on the redistribution of stress and control of deformation.

The preload was constant in the cable length analysis, and cable length of 2900, 3100, 3300, 3500, and 3700 mm were modelled to test the effect of anchorage depth. The excavation and support sequence was based on practical construction procedures, where the first step was the excavation of the roadway, and after that, anchor cables were installed and prestressed [23].

2.5 Stability Evaluation Indicators

To measure roadway stability and the performance of short anchor cable support quantitatively, several mechanical indicators were selected, such as stress, deformation and failure characteristics. Stress based indicators were the maximum tensile stress ($\sigma_{t,\max}$) and maximum compressive stress ($\sigma_{c,\max}$) that the surrounding rock had developed which is crucial in establishing regions that have a tendency to develop tensile cracks and compressive crushing under the loading of the excavations.

Deformation was quantified by the maximum resultant displacement:

$$u_{\max} = \max\sqrt{u_x^2 + u_y^2 + u_z^2} \tag{9}$$

which represents roadway convergence. Failure characteristics were evaluated using plastic zone distribution [24]. These indicators were extracted from the numerical results after support installation and stress stabilisation. Stability evaluation and support optimisation was performed through a detailed comparison of these indicators in varying simulation conditions, with lower stress concentration, diminished displacement, and smaller plastic zone extent representing a better roadway stability [25].

3 Results and Analysis

3.1 Stress Redistribution Characteristics under Variable Preload

Figure 1 shows the vertical stress distribution of the surrounding rock at various short anchor cable preloads. With 150 kN preload, tensile stress around the roadway is maximum at 0.514 MPa also compressive stress is maximum at 2.259 MPa. With the preload increase of 200 kN, the maximum tensile stress is reduced to 0.407 MPa, and the maximum compressive stress is raised to 2.445 MPa. Additional increases in preloads to 250 kN, 300 kN, and 350 kN lead to the maximum tensile stresses of 0.354 MPa, 0.323 MPa, and 0.316 MPa and the respective maximum compressive stresses rise to 2.539 MPa, 2.541 MPa, and 2.558 MPa.

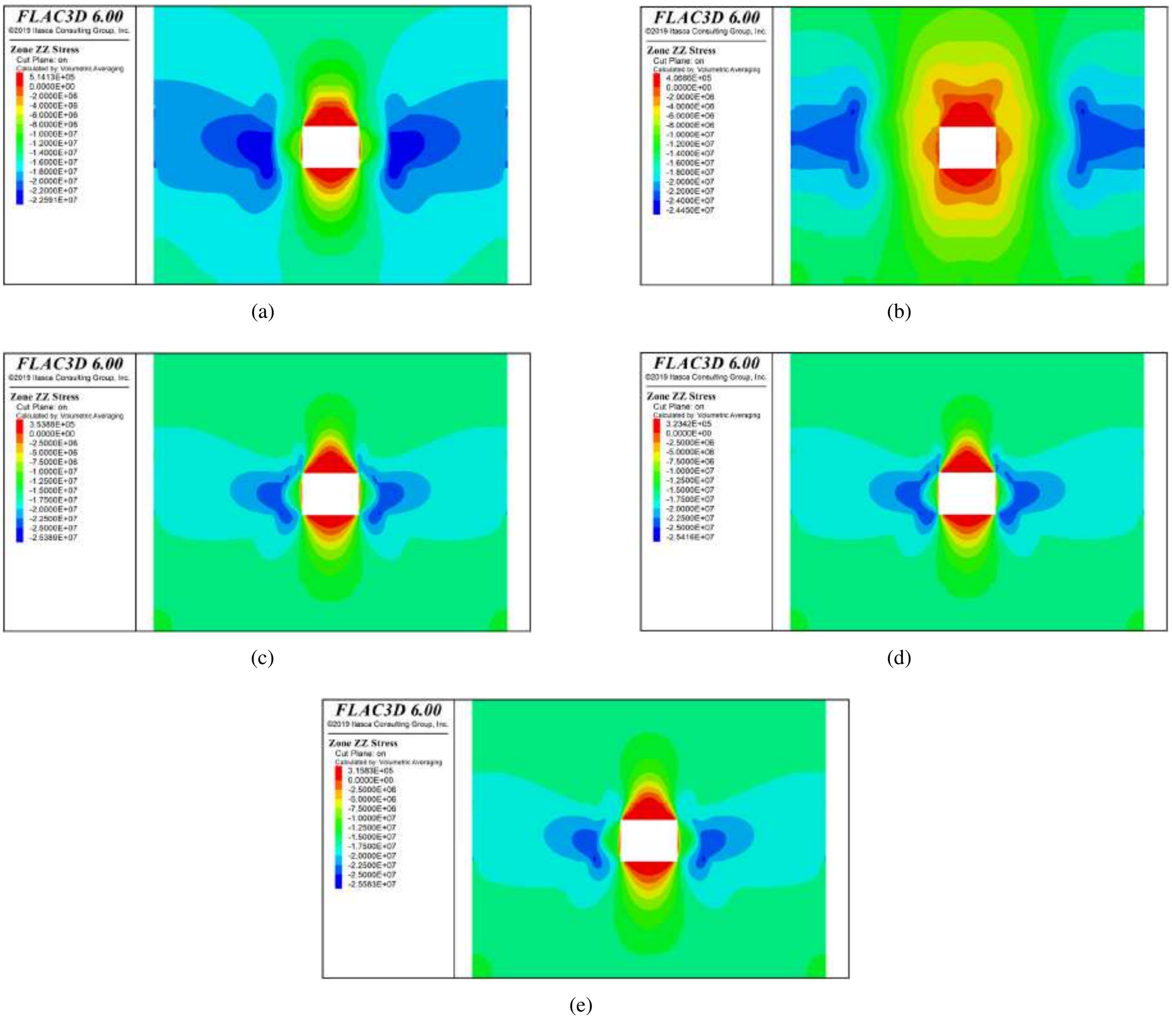

Figure 1. Vertical stress distribution diagram under different anchor cable preloads: (a) Preload is 150 kN of vertical stress distribution map, (b) Preload is 200 kN of vertical stress distribution map, (c) Preload is 250 kN of vertical stress distribution map, (d) Preload is 300 kN of vertical stress distribution map, and (e) Preload is 350 kN of vertical stress distribution map

Figure 2 indicates the quantitative relationships between the preloads of anchor cables and stress indicators. The maximum tensile stress is represented by solid line, whereas the dashed line represents the maximum compressive stress. As preload increases, the highest tensile stress decreases steadily, with a steep drop in the range of 150 kN to 300 kN, and then a slow steady increase after 300 kN. By comparison, the peak compressive stress rises exponentially between 150 kN and 250 kN and subsequently exhibits a non-linear increase with further preload increment.

The solid line represents the maximum tensile stress in Figure 2, whereas the dashed line represents the maximum compressive stress.

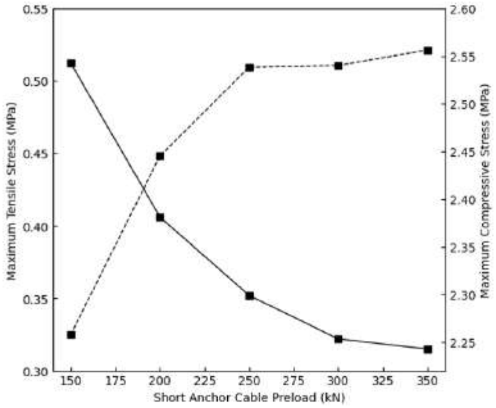

Figure 2. Relationship between maximum tensile stress and maximum compressive stress with short anchor cable preload

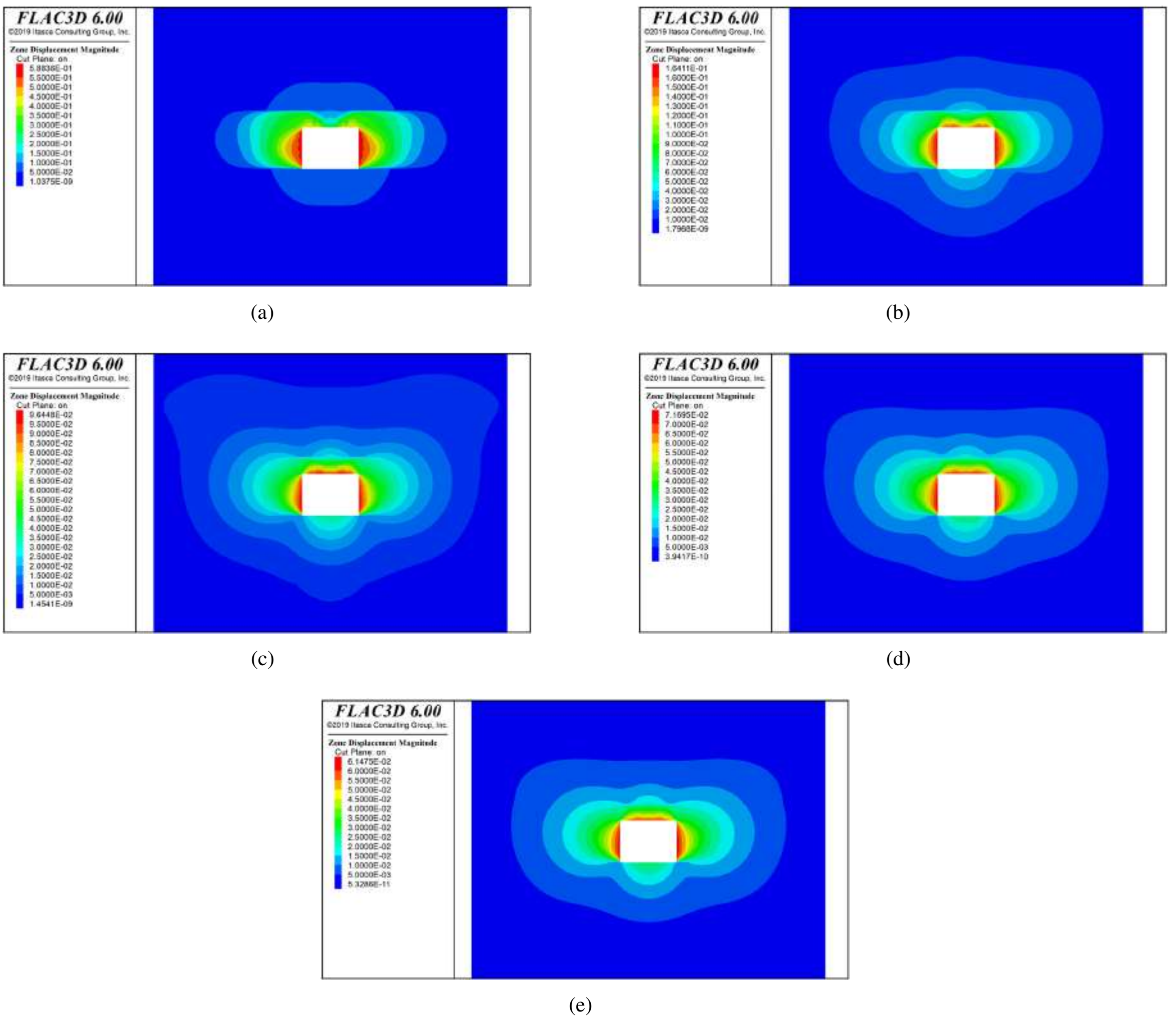

Figure 3. Displacement distribution under different anchor cable preload supports: (a) Preload for 150 kN displacement distribution map, (b) Displacement distribution diagram with a preload of 200 kN, (c) Displacement distribution diagram with a preload of 250 kN, (d) Displacement distribution diagram with a preload of 300 kN, and (e) Displacement distribution diagram with a preload of 350 kN

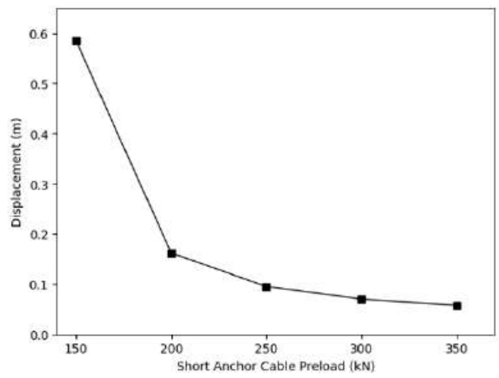

Figure 4. Relationship between displacement and preload of short anchor cable

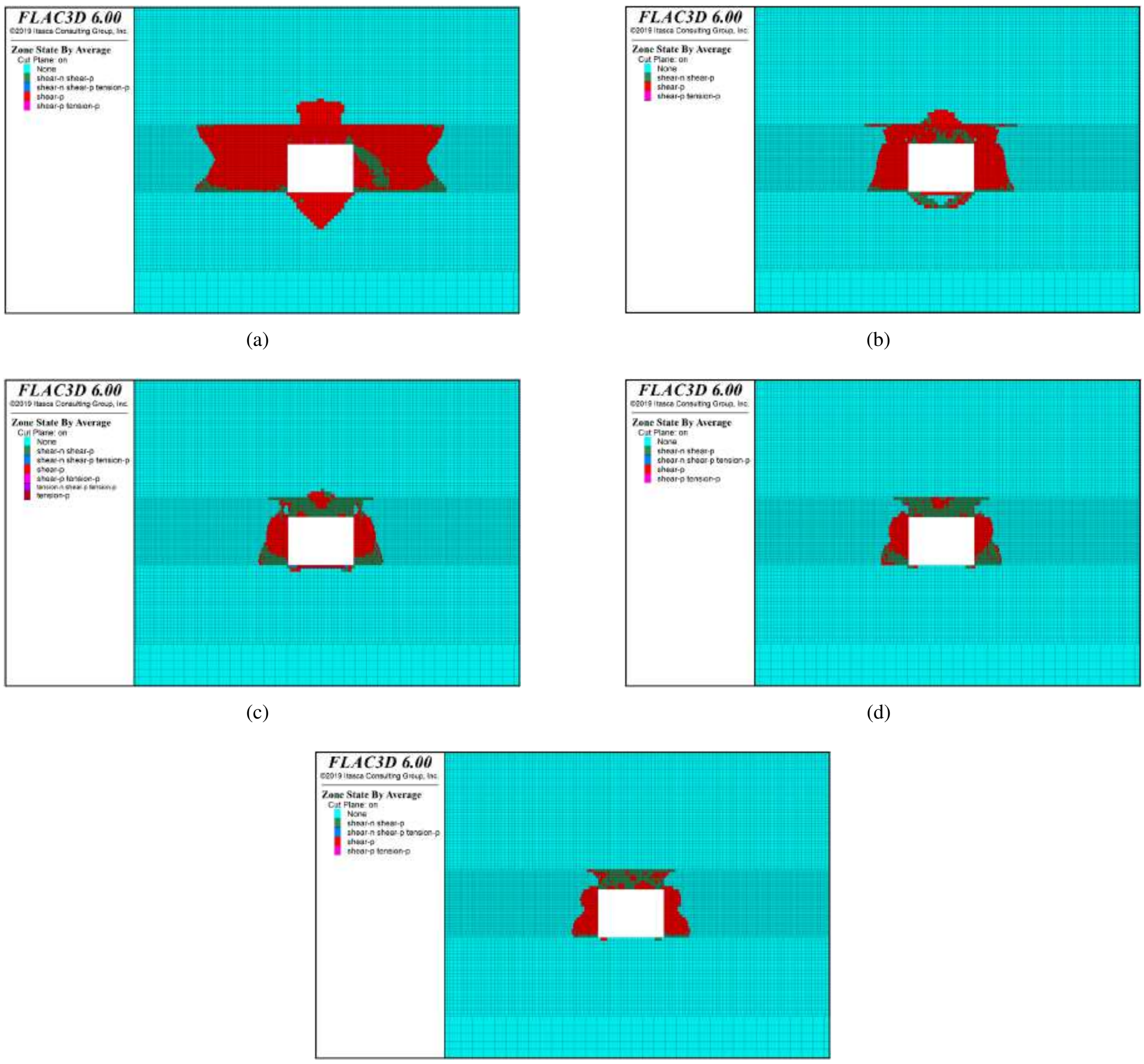

(a) (b) (c) (d) (e)

Figure 5. Distribution of the plastic zone under different anchor cable preloads: (a) Distribution of the plastic zone with a preload of 150 kN, (b) Distribution of the plastic zone with a preload of 200 kN, (c) Distribution of the plastic zone with a preload of 250 kN, (d) Distribution of the plastic zone with a preload of 300 kN, and (e) Distribution of the plastic zone with a preload of 350 kN

3.2 Deformation Behaviour Controlled by Anchor Cable Preload

Figure 3 shows the pattern of displacement of the surrounding rock at varied preloads of the anchor cable. A maximum roadway displacement of 0.588 m is obtained when the preload is 150 kN. As the preload is raised to 200 kN, the largest displacement reduces considerably to 0.164 m. Additional increase in preload to 250 kN, 300 kN and 350 kN decreases the maximum displacement to 0.096 m, 0.072 m and 0.061 m, respectively.

The correlation of maximum displacement and preload of anchoring cable is illustrated in Figure 4. The findings show that displacement reduces rapidly when the preload is increased by 150 kN to 200 kN, and the rate tends to be smaller when the preload is greater than 200 kN. This tendency indicates that further increase in preload is an effective way to increase the confinement of the surrounding rock, but that the marginal deformation control advantage decreases with higher preloads.

3.3 Plastic Failure Development under Different Preloads

Figure 5 depicts the distribution of the plastic zone of the surrounding rock at various anchor cable preloads. With a preload of 150 kN, a large plastic zone gradually forms around the roadway, especially on the two sides, with the maximum plastic zone depth of 9.56 m. The maximum plastic zone depth reduces to 4.14 m when the preload rises to 200 kN. At preloads of 250 kN, 300 kN and 350 kN, the maximum plastic zone depths further decrease to 2.74 m, 2.30 m, and 1.74 m, respectively.

The relationship between maximum plastic zone depth and the preload on the anchor cable is shown in Figure 6. The plastic zone depth decreases rapidly as preload increases from 150 kN to 250 kN, while the reduction becomes more gradual beyond 250 kN. These findings suggest that preload growth strongly inhibits the growth of plastic failure in the surrounding rock, and that the stabilisation effect of higher preload is clearly feasible.

This trend is further emphasised in Figure 7 where additional increases in preload increase compressive stress and increase shallow rock integrity, however, beyond 250 kN, further increases in preload offer minimal decrease in plastic zone extent. These findings justify the use of 250 kN as a suitable and cost-effective preload for controlling plastic failure.

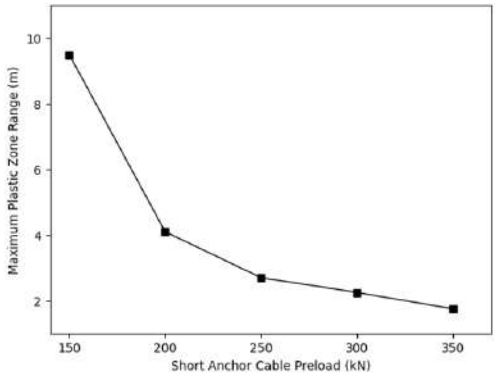

Figure 6. Plastic zone maximum value in range and short anchor cable preload relationship

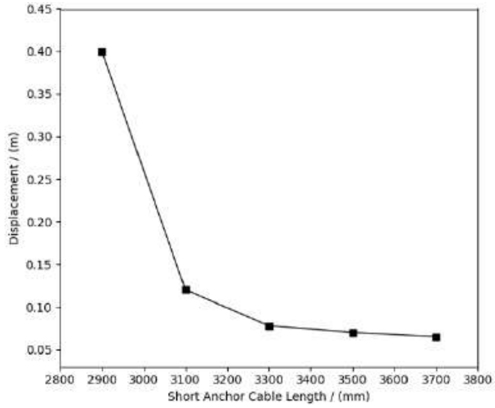

Figure 7. Displacement relationship with short anchor cable length diagram

3.4 Effect of Anchor Cable Length on Stress State of Surrounding Rock

As Figure 8 indicates, the distribution of vertical stress on the surrounding rock is different at various short anchor cable lengths. With a cable length of 2900 mm, the maximum compressive stress is 2.364 MPa and the maximum tensile stress is 0.3483 MPa. With increased length to 3100 mm and 3300 mm, tensile stress becomes minimal at 0.3469 MPa and 0.3441 MPa, respectively, whereas compressive stress is at the maximum at 2.457 MPa and 2.537 MPa, respectively. Additional increments in cable length to 3500 mm and 3700 mm result in tensile stresses of 0.3439 MPa and 0.3391 MPa and compressive stresses of 2.539 MPa and 2.541 MPa.

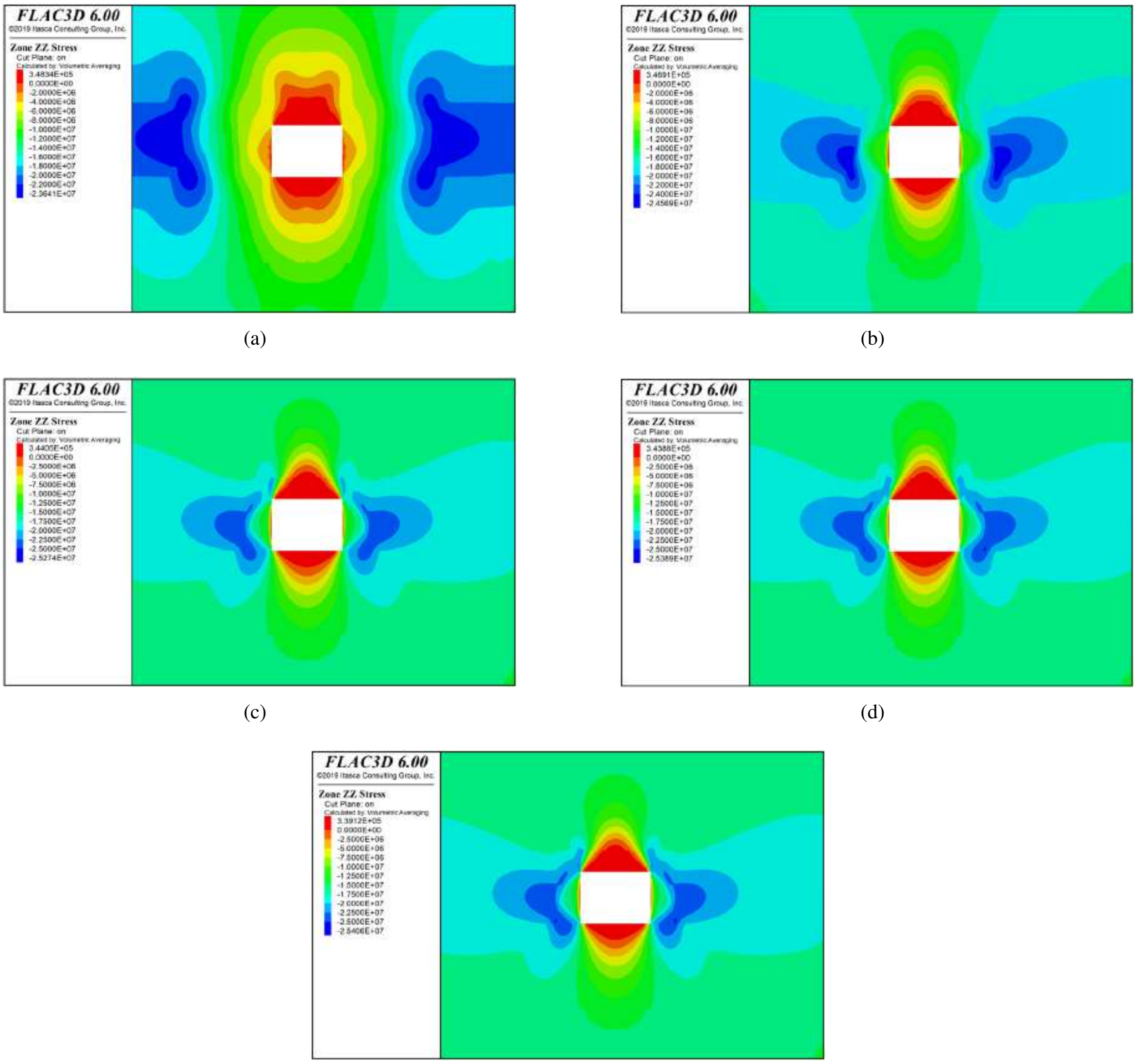

(a) (b) (c) (d) (e)

Figure 8. Vertical stress distribution diagram under different short anchor cable lengths: (a) Length is 2900 mm of vertical stress distribution map, (b) Length is 3100 mm of vertical stress distribution map, (c) Length is 3300 mm of vertical stress distribution map, (d) Length is 3500 mm of vertical stress distribution map, and (e) Length is 3700 mm of vertical stress distribution map

As shown in Figure 9, the maximum tensile stress is represented by the solid line, while the dashed line represents the maximum compressive stress. Tensile stress decreases and compressive stress increases with a longer length of the anchor cable. The difference is more pronounced when the cable length is increased between 2900 mm and 3300 mm and the change in stress becomes less significant after 3300 mm.

In Figure 9, the solid line represents the maximum tensile stress, while the dashed line represents the maximum compressive stress.

3.5 Influence of Anchor Cable Length on Deformation and Plastic Zone

The distribution of displacement at various lengths of the anchor cable is given in Figure 10. Its maximum displacement is 0.400 m at length of 2900 mm and then rapidly decreases to 0.124 m and 0.080 m at length of 3100 mm and 3300 mm respectively. As the cable length extends further to 3500 mm and 3700 mm the maximum displacement reduces somewhat to 0.072 m and 0.067 m.

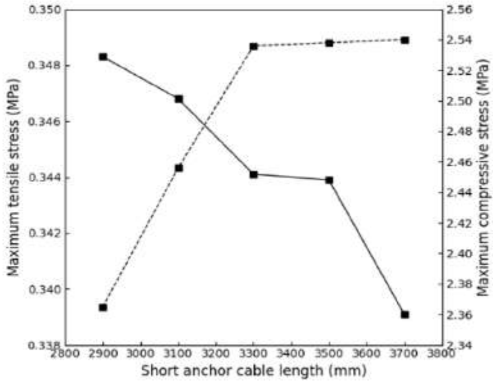

Figure 9. Relationship between maximum tensile and compressive stresses and short anchor cable length

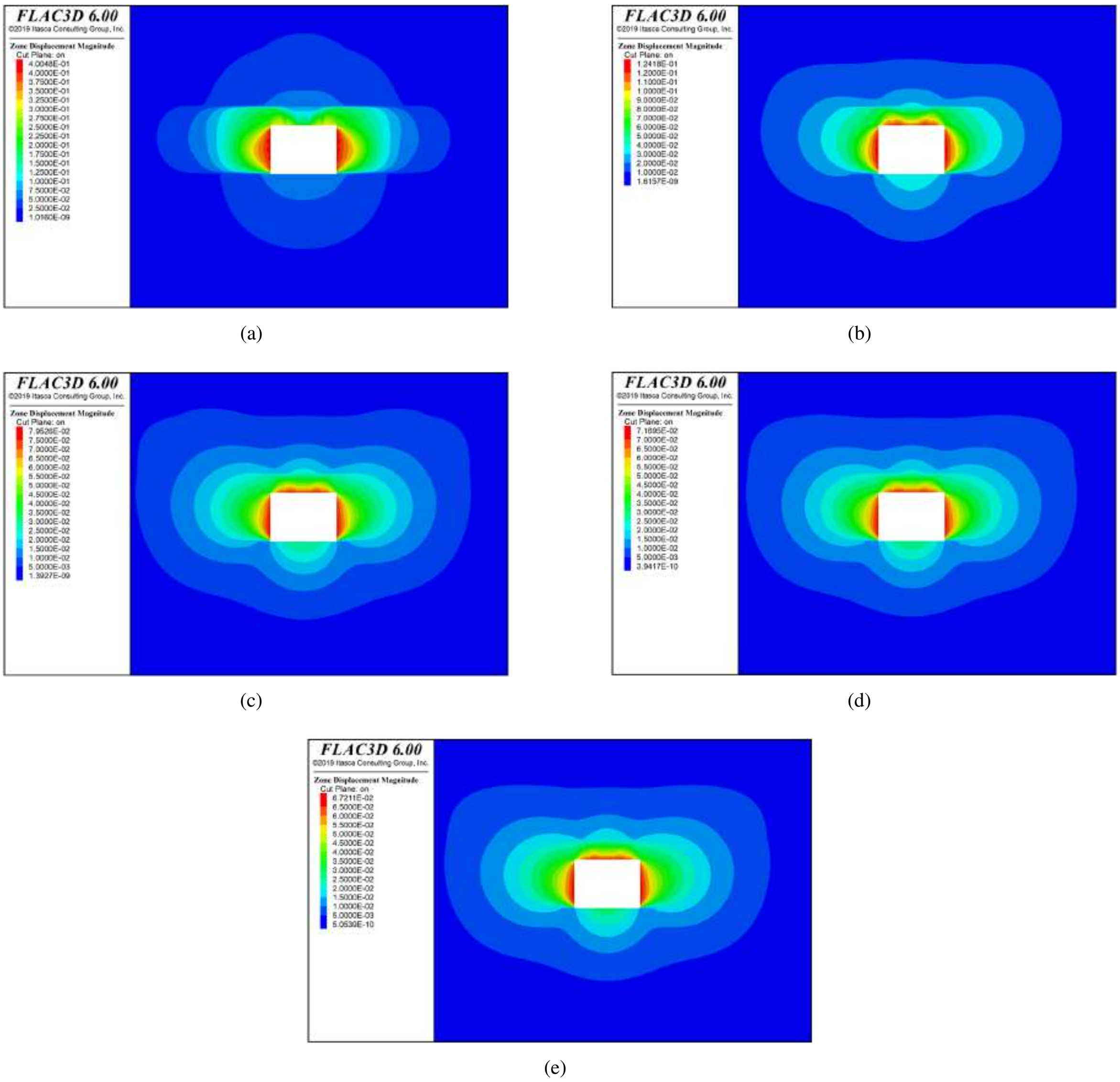

(a) (b) (c) (d) (e)

Figure 10. Displacement distribution under different short anchor cable lengths: (a) Displacement distribution diagram with a length of 2900 mm, (b) Displacement distribution diagram with a length of 3100 mm, (c) Displacement distribution diagram with a length of 3300 mm, (d) Displacement distribution diagram with a length of 3500 mm, and (e) Displacement distribution diagram with a length of 3700 mm

The distributions of plastic zone are presented in Figure 11 under varied cable length. The maximum plastic zone depth is 8.04 m when the length is 2900 mm. This value is reduced to 3.49 m, 2.34 m, 2.20 m and 2.11 m as the cable length is increased to 3100 mm, 3300 mm, 3500 mm and 3700 mm respectively. As Figure 12 confirms, the plastic zone depth declines at an increasing rate to 3300 mm and then stabilises.

The findings show that both preload on the anchor cable and its length have a significant impact on the distribution of stress, deformation, and plastic failures development. As preload is increased, tensile stress, displacement, and plastic zone depth are decreased whereas compressive stress increases, but further increases yield no improvement above 250 kN.

Correspondingly, stability is aided by cable length, with the best performance being realised at 3300 mm. Generally, additional increases provide limited benefits. Based on stability and efficiency of construction and economic considerations, a short anchor cable preload of 250 kN and a cable length of 3300 mm are selected as the best parameters demonstrated by the studied roadway. These settings effectively control plastic failure and deformation while avoiding unnecessary cost and construction complexity.

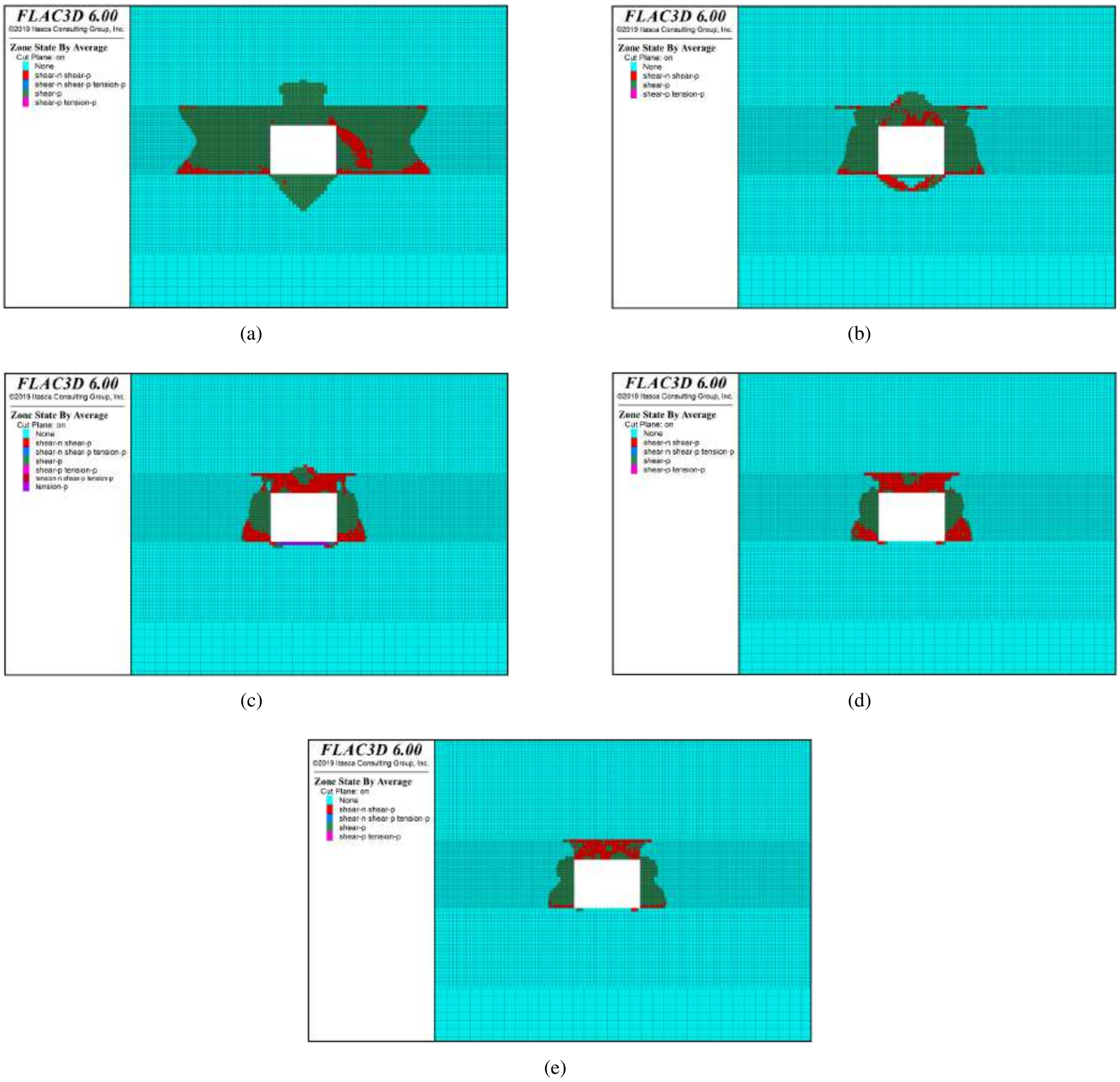

Figure 11. Distribution of the plastic zone under different anchor cable lengths: (a) Distribution of the plastic zone with a length of 2900 mm, (b) Distribution diagram of the plastic zone with a length of 3100 mm, (c) Distribution diagram of the plastic zone with a length of 3300 mm, (d) Distribution diagram of the plastic zone with a length of 3500 mm, and (e) Distribution diagram of the plastic zone with a length of 3700 mm

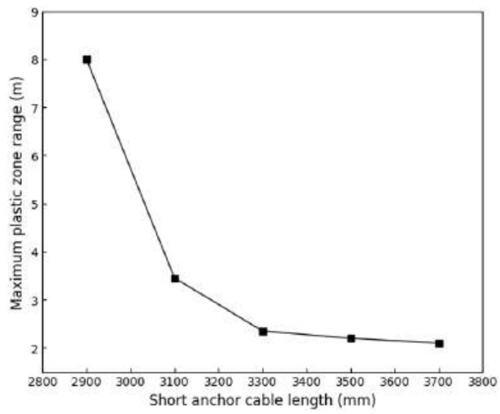

Figure 12. Relationship between the maximum value of the plastic zone and the length of the short anchor cable

4 Discussion

The numerical results clearly demonstrate that anchor cable preload and length are key design parameters that govern stress redistribution, deformation behavior, and plastic failure evolution of the surrounding rock. These results are consistent with the current knowledge about prestressed anchorage in rock engineering, in which pretension force has been shown to affect stress field modification and deformation control in excavation support systems [26]. With increasing preload of 150 kN to 350 kN, limiting tensile stress monotonically reduced and maximum compressive stress increasing. This reaction is an increase in the confinement of the shallow surrounding rock. The first sudden decrease of tensile stress to 300 kN indicates that prestress is successful in shifting the stress state out of tension-dominating and into compression-controlled, an essential step towards eliminating crack formation and propagation.

However, beyond 300 kN, the stress indicators stabilise, indicating diminishing returns from further increases in preload. This plateau effect is compatible with mechanical interpretation of equivalent support force, it reaches a point were making the surrounding rock as close as possible to a quasi-equilibrium stress state, further prestress reduces redistribution because the rock mass can be mobilised to make the rock mass limited. The role of prestress can also be explained by the displacement responses under different preloads. Optimal roadway movement displacement declines considerably with preload to a point at 200 kN, beyond which the downward trend becomes flattened.

The pattern can be explained by the mechanical activation of near field rock confinement: low preload conditions cause the further prestress to annul fractures and diminish loosened areas, causing great deformation reductions. At increased preloads, a large part of the potential fracture closing and stress-transfer has already taken place, and the additional contribution to displacement is smaller. This reinforces the idea of a threshold preload beyond which only marginal improvements can be made- an idea that is also reflected in realistic design advice that suggests the use of balanced prestresses to prevent excessive tensioning which may not result in meaningful increases in performance. The depth of the plastic zone decreases very rapidly with increase in preload till reaching depth of 250 kN and thereafter decreases more slowly. The relations which illustrate this are given in Figure 6 and Figure 7, which show that suppressing plastic failure is more effective with a preload to a given threshold beyond which there are only marginal gains.

In terms of engineering, this underpins the selection of 250 kN as a cost-effective and effective preload to be used to control deformation, suppress plastic failure and to ensure construction feasibility. Change in the anchor cable length created similar transitional behavior. Longer cables minimised tensile stress and displacement as well as maximised compressive stress and minimise plastic zone depth.

The most remarkable changes fall in the 2900 mm to 3300 mm range after which the changes become less pronounced. This means that there is an effective anchorage depth that gives maximum transfer of load to rock mass, further increases in length add very little to redistribution of stress or control of deformation. In prestressed anchor systems, longer cable lengths permit the prestress to be conveyed deeper in the rock mass, although beyond the extent of influence of the plastic and loosened rock, the extra length is inelastic regions and thus has little effect [27].

Overall, these research findings indicate that not only specification of preload and length is required, but also that prestress should be mobilised and held in the rock mass, a factor that can also be used to further narrow the optimum values found in this study.

5 Practical Implications

The findings are a direct practical recommendation in the field of underground roadway support design. First, preload needs to be optimised, not maximised. A prestress level of about 250 kN provides a significant redistribution of stress and deformation control and does not require excessive energy input, installation complexity, and is economically inefficient. Too much prestress can raise construction cost, but not in a proportionate mechanical gain. Second, the length of anchor cables should allow penetration across the shallow plastic area through competent rock strata. The effective anchorage depth of about 3300 mm identified and provides an efficient transfer of loads and mobilisation of deeper confinement. Beyond this length, there is no substantial increase in stability to compensate for a decrease in the efficiency of the construction and the economy of materials.

Third, preload and cable length must be considered in a coordinated manner. Isolated parameter optimisation does not always give balanced performance. The hybrid design increases mechanical stability, and it is feasible to construct.

However, the selection of parameters is site-specific. The differences in rock mass characteristics, joint development and long-term prestress loss need to be calibrated by field monitoring so that they can be effectively used in various geological settings.

6 Conclusions

The research examined the effect of preload and length of short anchor cables on the stress distribution, deformation behaviour and plastic failure development of the surrounding rock in a roadway environment through numerical simulations. The findings indicate that preload and cable length are vital factors when it comes to stabilisation of the rock mass and control of plastic deformation. The preloading of anchor cables is effective in lessening the maximum tensile stress, displacement and depth of plastic zone and enhancing compressive stress of the adjacent rock. However, the tensile stress and plastic zone reduction show a decreasing marginal benefit beyond a preload of about 250 kN and suggests that increasing levels of prestress can offer marginal benefit and may not be cost effective. Similarly, increasing anchor cable length improves the stability of the surrounding rocks by decreasing tensile stress and displacement and more effectively contains the plastic zones. The greatest changes are made as the cable length grows beyond 2900 mm up to 3300 mm, after which the stabilising effect levels off, indicating that there is likely a certain optimal anchorage depth to stress transfer.

These results have brought to focus the role of preload and cable length considered in a coordinated way to realize efficient and cost-effective roadway support. Using the combined evaluation of stress redistribution, deformation control, and plastic failure suppression, a preload of 250 kN on the short anchor cable along with a cable length of 3300 mm has been found to represent the best support configuration of the investigated roadway. This combination is effective in balancing mechanical performance, construction efficiency and economic consideration, which offer a practical guideline to such underground support projects. The research contributes to the knowledge of prestressed anchor behaviour in rock engineering and highlights the importance of choosing the right design parameters to increase the stability of underground excavation. Future studies should be directed towards field validation and inclusion of variable geological conditions and jointed rock behaviour as well as loss of prestress in the long-term to further hone anchor cable design and ensure robust support in a wide variety of rock mass environments.

Author Contributions

Conceptualization, R.S. and R.W.; methodology, R.S. and R.W.; software, R.S. and R.W.; validation,R.S.; formal analysis, R.S.; resources, R.W.; data curation, R.S.; writing—original draft preparation, R.S.; writing—review and editing, R.W. and B.J.; visualization, R.S.; supervision, R.W.; project administration, R.S. and R.W.; funding acquisition, R.W. All authors have read and agreed to the published version of the manuscript.

Data Availability

All data generated or analysed during this study are included in this published article.

Conflicts of Interest

On behalf of all authors, the corresponding author affirms that there is no conflicts of interest exists.

References

[1] Q. L. Yun, X. H. Wang, W. Jing, W. B. Zhang, X. X. Wei, and J. H. Wang, "Characteristics of deformation and damage of surrounding rock along the top roadway in the working face of an isolated island and its evolution law," *Sci. Rep.*, vol. 14, no. 1, p. 15092, 2024. https://doi.org/10.1038/s41598-024-63246-x

[2] S. Pu, R. Wu, S. Wu, L. Cao, and Z. Ren, "Analysis of deformation characteristics and failure mechanism of interbedded surrounding rock tunnels based on principal stress difference," *Int. J. Geomech.*, vol. 24, no. 9, 2024. https://doi.org/10.1061/IJGNAI.GMENG-9558

[3] N. Abbas, K. Li, Y. Fissha, W. Lei, M. Emad, N. S. Chandrahas, J. Khatti, B. Taiwo, M. Sazid, Z. Gebrehiwot, S. Hosseini, and N. R. Cheepurupalli, "Stress-deformation and stability challenges in Himalayan tunnels:

Impact of geological discontinuities," *Discov. Mater.*, vol. 4, no. 1, p. 72, 2024. https://doi.org/10.1007/s43939-024-00144-z

[4] Z. Luo, Z. Ru, L. Zheng, Z. Zhang, Z. Zhang, J. Xie, L. Zhang, and L. Ren, "Analytical solution and factors influencing the tunnel plastic zone under a nonuniform stress field," *KSCE J. Civ. Eng.*, vol. 28, no. 7, pp. 3016–3032, 2024. https://doi.org/10.1007/s12205-024-1645-8

[5] C. Yuan, J. Lu, Y. Jiang, J. Xiao, S. Chen, J. Cui, and Z. Qi, "Influence of tunnel excavation on the magnitude and rotation angle of principal stress in surrounding rock," *Sci. Rep.*, vol. 14, no. 1, p. 25512, 2024. https://doi.org/10.1038/s41598-024-76030-8

[6] M. Wang, A. Shi, H. Li, F. Yuan, and J. Zhou, "Deformation and failure mechanism of surrounding rock mass in a large-scale underground powerhouse under high in-situ stress," *Results Eng.*, vol. 21, p. 101638, 2024. https://doi.org/10.1016/j.rineng.2023.101638

[7] W. Frenelus, H. Peng, and J. Zhang, "An insight from rock bolts and potential factors influencing their durability and the long-term stability of deep rock tunnels," *Sustainability*, vol. 14, no. 17, p. 10943, 2022. https://doi.org/10.3390/su141710943

[8] Y. Yang, L. Meng, and T. Zhang, "Full anchor cable support mechanism and application of roadway with thick soft rock mass immediate roof," *Appl. Sci.*, vol. 13, no. 12, p. 7148, 2023. https://doi.org/10.3390/app13127148

[9] R. Shan, S. Xiao, Y. Li, X. Zhao, T. Han, and S. Zhang, "Study on numerical simulation and mechanical properties of anchor cable with C-shaped tube subjected to shearing," *Sci. Rep.*, vol. 14, no. 1, p. 7425, 2024. https://doi.org/10.1038/s41598-024-58085-9

[10] P. Li, Y. Chen, J. Huang, X. Wang, J. Liu, and J. Wu, "Design principles of prestressed anchors for tunnels considering bearing arch effect," *Comput. Geotech.*, vol. 156, p. 105307, 2023. https://doi.org/10.1016/j.compgeo.2023.105307

[11] J. Terron-Almenara, E. Skretting, K. G. Holter, and A. H. Høien, "Design of rock support in hard and layered rock masses using a hybrid method: A study based on the construction of the new Skarvberg tunnel, Norway," *Rock Mech. Rock Eng.*, vol. 57, no. 12, pp. 10 491–10 532, 2024. https://doi.org/10.1007/s00603-024-04082-3

[12] R. Shan, H. Bai, Y. Li, H. Wu, P. Sun, X. Zhao, H. Dou, and H. Wang, "Analytical solution of surrounding rock stress and plastic zone of rectangular roadway under non-uniform stress field," *Sci. Rep.*, vol. 14, no. 1, p. 27482, 2024. https://doi.org/10.1038/s41598-024-79221-5

[13] X. Tong, R. Shan, N. Liu, D. Liu, and Y. Wei, "Experimental study on the shear performance of an anchor cable with a C-shaped tube anchored flat structural plane," *Sci. Rep.*, vol. 13, no. 1, p. 797, 2023. https://doi.org/10.1038/s41598-023-28105-1

[14] J. Xu and Y. Wang, "Stability analysis and support design methods for rock foundation pit with combination of structural plane and karst cave," *Adv. Civ. Eng.*, vol. 2022, p. 5662079, 2022. https://doi.org/10.1155/2022/5662079

[15] A. Liu, H. Li, F. Lu, and M. Niu, "Numerical simulation with FLAC3D on excavation process of underground powerhouse of Kaluma Hydropower Station," in *Advances in Frontier Research on Engineering Structures*. Springer, 2023, pp. 211–217. https://doi.org/10.1007/978-981-19-8657-4_19

[16] H. Bakhshan, E. Oñate, and J. M. Carbonell i Puigbó, "A review of the constitutive modelling of metals and alloys in machining process," *Arch. Comput. Methods Eng.*, vol. 31, no. 3, pp. 1611–1658, 2024. https://doi.org/10.1007/s11831-023-10026-x

[17] Y. I. Park, J. S. Cho, and J. H. Kim, "Numerical and experimental investigation of quasi-static crushing behaviors of steel tubular structures," *Materials*, vol. 15, no. 6, p. 2107, 2022. https://doi.org/10.3390/ma15062107

[18] C. F. Hsu, Y. H. Tsai, Y. R. Chen, Y. F. Li, and S. L. Chen, "Normalized analysis of deformation for deep excavation diaphragm walls under different neighboring building conditions," *Results Eng.*, vol. 22, p. 102155, 2024. https://doi.org/10.1016/j.rineng.2024.102155

[19] L. Yan, Z. Xiang, W. Xu, R. Wang, and H. Ji, "Numerical simulation of mechanical properties of irregular columnar jointed rock mass," *Front. Phys.*, vol. 10, p. 836286, 2022. https://doi.org/10.3389/fphy.2022.836286

[20] Y. Yang, L. Meng, and T. Zhang, "Full anchor cable support mechanism and application of roadway with thick soft rock mass immediate roof," *Appl. Sci.*, vol. 13, no. 12, p. 7148, 2023. https://doi.org/10.3390/app13127148

[21] Y. Liu, P. Zheng, and P. Wang, "Multi-factors influence of anchorage force on surrounding rock under coupling effect of creep rock mass and bolt/cable," *Geomatics Nat. Hazards Risk*, vol. 12, no. 1, pp. 328–346, 2021. https://doi.org/10.1080/19475705.2021.1872717

[22] W. Chen, C. Hong, X. Chen, G. Luo, and D. Su, "Comparative analysis of anchor cables in pullout tests using distributed fiber optic sensors," *Can. Geotech. J.*, vol. 60, no. 12, 2023. https://doi.org/10.1139/cgj-2022-0455

[23] S. Zhou, Y. Jin, Z. Tian, C. Zou, H. Zhao, and Z. Miao, "Exploring the feasibility of prestressed anchor cables as an alternative to temporary support in the excavation of super-large-span tunnel," *Railw. Eng. Sci.*, vol. 32, no. 3, pp. 344–360, 2024. https://doi.org/10.1007/s40534-024-00340-w

[24] M. Askaripour, A. Saeidi, A. Rouleau, and P. Mercier-Langevin, “Rockburst in underground excavations: A review of mechanism, classification, and prediction methods,” *Undergr. Space*, vol. 7, no. 4, pp. 577–607, 2022. https://doi.org/10.1016/j.undsp.2021.11.008

[25] J. Yao, N. Jiang, Y. Yao, C. Zhou, and Y. Yang, “Instability mechanism of layered surrounding rock tunnels affected by layer thickness under dynamic and static loads,” *Alex. Eng. J.*, vol. 105, pp. 471–484, 2024. https://doi.org/10.1016/j.aej.2024.07.031

[26] W. Yu, B. Wang, X. Zi, X. Guo, and Z. Wang, “Effect of prestressed anchorage system on mechanical behavior of squeezed soft rock in large-deformation tunnel,” *Tunn. Undergr. Space Technol.*, vol. 131, p. 104782, 2023. https://doi.org/10.1016/j.tust.2022.104782

[27] L. Wang, “Secondary anchorage and prestress loss of fractured strand in PT beams,” in *Strand Corrosion in Prestressed Concrete Structures*. Springer Nature Singapore, 2023, pp. 167–191. https://doi.org/10.1007/978-981-99-2054-9_7